

**Effect of Different Micro Grain Sizes of Sedimentary Rocks on Uranium Leachability****H.A.S. Aly***Physics Department, Faculty of Women for Arts, Science and Education, Ain Shams University, Heliopolis11757, Cairo, Egypt***ABSTRACT**

Effects of different micro grain sizes of sedimentary rock samples on uranium leaching quantities have been investigated. Four selected samples under drawn leaching process using sulfuric acid were used. Activity concentrations of uranium isotopes  $^{238}\text{U}$ ,  $^{235}\text{U}$  and  $^{234}\text{U}$  were determined for the original samples, of different grain sizes, and their corresponding uranium bearing solutions at the same leaching conditions (automatic stirring for 1h and one week soaking time). The pH and temperature of the bearing solutions have been determined and Uranium leachability trend has been investigated. Obtained results indicate that uranium leachability depends on sample rock type. Also it was found that  $^{234}\text{U}$  is the more leaching isotope than the  $^{238}\text{U}$  and  $^{235}\text{U}$ .

**Keywords:** Uranium leachability, Uranium isotopes, Uranium bearing solutions.

**Introduction**

Radiographic measurements of uranium activity in nature have great importance. Primordial uranium consists of three isotopes,  $^{238}\text{U}$  and  $^{234}\text{U}$  from the uranium series and  $^{235}\text{U}$  from the actinium series. In nature, an imbalance between  $^{234}\text{U}$  and  $^{238}\text{U}$  may exist due to alpha particle withdraw from the decay of  $^{238}\text{U}$  that increases the availability of  $^{234}\text{U}$  for transport through geological processes (Maria *et al.*, 2009).

In a typical sample of natural uranium, most of the weight (99.27%) consists of atoms of  $^{238}\text{U}$ . About 0.72% of the weight consists of atoms of  $^{235}\text{U}$ , and a very small amount (0.0055% by weight) is  $^{234}\text{U}$  (U.S.EM 2001).

Analyses of natural and man-made radionuclides in environmental samples are complex procedures requiring multiple steps of preparation, leaching or total dissolution, separation and measurement. One of the most important requirements of such an analytical procedure is to ensure complete dissolution or reproducible leaching of the analyte from the sample (Benedik *et al.*, 1999).

Uranium is more closely associated with iron and manganese, probably adsorbed to or co-precipitated with oxides of Fe, Mn and Al (Cecilia *et al.*, 2000), and it can be extracted and chemically converted into uranium dioxide ( $\text{UO}_2$ ) or other chemical forms (Maria *et al.*, 2009).

Uranium leaching strongly depends on the mineral structure of the sample (Benedik *et al.*, 1999). Based on their solubility in dilute sulfuric acid solutions, minerals are subdivided into three groups: 1. Insoluble: quartz, accessory minerals and solid bitumen; 2. Solubility resistant: feldspars, hydromicas, montmorillonite, kaolinite, muscovite, sericite, as well as relics of metamorphic and clay rock; 3. Soluble: calcite, dolomite, limonite, biotite and epidote. The majority of uranium minerals occurring in sandstone deposits are in the soluble group (IAEA, 2001).

The present work intended to investigate the effect of sample characteristics and their grain sizes as well as their leaching quantities on the detected uranium using gamma spectrometry, the different samples were selected and chosen with the consideration of the above literatures notes.

**2. Sampling:****2.1 Sample characteristics:**

Studied samples have been collected from Um Bogma, southwestern Sinai, Egypt. It is preferable to collect the representative samples from different localities. Table.1 shows the studied samples characteristics.

**Table 1:** Lithostratigraphic profile of the studied samples.

Formation	Sample	Member	Main lithology and environment
Um Bogma Formation	S1	Upper dolomite Sandstone	Sandstone with shale intercalations, coal in the upper part.
	S2	Sandy dolomite	Yellow to pink dolostone with occasional yellow shale, warm shallow – marine environment unconformity
	S3	Marly dolostone, siltstone	Karstified member, siltstone representing soil cover
	S4	Lower dolostone	Extensively Karstified dolomitic rocks with intrakarstic product housing manganese ores and caliche nodules.

These localities are known as, Um Bogma Formation (UB) (8m thick), which is a radioactive rock unit and is consisted of argillaceous sediments and dolostones. The Cambrian rocks (sandstones) are unconformably overlying by lower carboniferous 360 m.y (Tucker, 2003).

## 2.2. Sample preparation:

Collected samples were dried, each dried sample was divided by quartering, pulverized to different grain sizes 63, 33 and 8  $\mu\text{m}$  now each sample with different grain size has been homogenized, finally 200 ml volume of each sample with different grain sizes has been weighed and transferred to polyethylene Marinelli beaker.

## 2.3 Bearing Solution preparation:

Leaching processes were carried out on 100 g from each sample at different grain sizes, using 30%  $\text{H}_2\text{SO}_4$  under the conditions of 1h stirring, then leachates were separated (filtered) after one week of soaking and packed in 200 ml polyethylene Marinelli beakers. At the initial stage of sulfuric acid leaching, the hexavalent form of uranium is by far the dominant species to enter solution. Should the pH value be reduced below 2 then  $\text{U}^{4+}$  ions enter the solution, though to a much reduced degree than  $\text{U}^{6+}$  ions (IAEA, 2001). In the present work the pH of produced solution ranges from 1.9 to 2.1 and the temperature from 26 to 29 °C.

## 3. Experimental Techniques:

### 3.1. HP-Ge detector:

The samples were analyzed non-destructively, using gamma- ray spectrometry with a high-purity germanium (HP-Ge) detector. This detector has a relative efficiency of approximately 50% of the 3"x 3" NaI(Tl) crystal efficiency, with a resolution of 1.90 keV and a peak/ Compton ratio of 69.9:1 at the 1.33 MeV gamma-ray transition of  $^{60}\text{Co}$ . The detector is coupled to conventional electronics and connected to a multi-channel analyzer (MCA) card installed in a PC. The detector is shielded from the background radiation, using a 10-cm thick lead shield, internally lined with a 2-mm thick copper foil. The soft ware program MAESTRO-32 was used to accumulate and analyze the data. The system is calibrated for energy to display gamma-ray photo-peaks between 63 and 3000 keV. The efficiency calibration was performed by using three well-known reference materials obtained from the International Atomic Energy Agency for the U, Th and K activity measurements: RGU-1, RGTh-1, and RGK-1 respectively (IAEA, 1987).  $^{238}\text{U}$  activity was determined indirectly from analyzing the gamma rays emitted by its daughter product ( $^{234\text{m}}\text{Pa}$ ) determined from the 1001 keV photo-peak, (Sutherland and deJong, 1990),  $^{235}\text{U}$  activity was determined by its gamma ray photo-peaks: 143.8, 163.4, 185.7 and 205.3 keV (Ramebäck *et al.*, 2010) and the  $^{234}\text{U}$  activity was determined from its gamma ray photo-peak 120.9 keV (Yokoyama *et al.*, 2008 & Yücel *et al.*, 2010).

### 3.2. EDX instrument:

Element contents for the different samples with different grain sizes have been measured and listed in Table. 7 for this operation Scanning Electron Microscope connected to Energy Dispersive X-Ray System (SEM/EDX), using EDX instrument of: Gain factor: 49.996, Live time: 30 Seconds, System resolution: 129.48 eV and Accelerating voltage: 20.00 KV.

## 4. Methodology:

### 4.1. Gamma measurements:

Samples are measured by  $\gamma$ -spectrometry using hyper pure germanium detector to determine the activity concentrations in Bq/kg for  $^{238}\text{U}$ ,  $^{235}\text{U}$  and  $^{234}\text{U}$ .

For radiometric analysis, the samples were subjected to gamma- ray spectrometric analysis. After each sample counting, an empty polyethylene Marinelli beaker was placed in the detection system, for a counting period of 48 h, in order to collect the background count rates.

### 4.2. Radioactivity counting:

The net area count, after background corrections in each photo-peak, was used in the computation of the activity concentration (C) in  $\text{Bq kg}^{-1}$  for each of the uranium isotopes in the samples using the following expression (Jibiri *et al.*, 2007):

$$C(\text{Bq Kg}^{-1}) = \frac{C_n}{\varepsilon P_\lambda M_s} \quad (1)$$

Where  $C_n$  is the count rate under each photo- peak due to each radionuclide,  $\varepsilon$  is the detector efficiency for the specific  $\gamma$ -ray,  $P_\lambda$  is the absolute transition probability of the specific  $\gamma$ -ray and  $M_s$  is the mass of the sample (kg).

## Results and Discussions

### 5.1. Activity concentrations:

Activity concentration values in  $\text{BqKg}^{-1}$  of  $^{238}\text{U}$ ,  $^{235}\text{U}$  and  $^{234}\text{U}$  for different measured solid samples are listed in Table. 2.

Results of gamma measurements of the solid samples show that the highest uranium activities are noticed in the two samples S1 (upper sandstone with shale rock) and S4 (lower dolomitic rock) while the others two samples S2 & S3 (middle members of the studied Um Bogma formation) are characterized by less uranium activities than S1 and S4. Activity ratios of  $^{238}\text{U} / ^{235}\text{U}$  and  $^{238}\text{U} / ^{234}\text{U}$  are listed in Table.3. Where  $^{238}\text{U} / ^{235}\text{U}$  ratio range from 20.53 to 22.14, while  $^{238}\text{U} / ^{234}\text{U}$  ratio is nearly equal to unity for the different studied samples as shown in Table.3, thus assuming secular equilibrium between  $^{238}\text{U}$  and  $^{234}\text{U}$ .

While the corresponding bearing solutions activity concentration measurements values in  $\text{BqL}^{-1}$  of  $^{238}\text{U}$ ,  $^{235}\text{U}$  and  $^{234}\text{U}$  are listed in Table. 4.

Uranium isotopes measurements of bearing solutions prepared from different samples at different grain sizes show different levels of uranium leaching quantities according to sample rock type, also it has been noted that the leaching quantities of  $^{234}\text{U}$  was more than the other isotopes  $^{238}\text{U}$  and  $^{235}\text{U}$ . Activity ratios of  $^{238}\text{U} / ^{235}\text{U}$  and  $^{238}\text{U} / ^{234}\text{U}$  are listed in Table.5. Where  $^{238}\text{U} / ^{235}\text{U}$  ratio ranges from 20.15 to 22.29 where  $^{238}\text{U} / ^{234}\text{U}$  deviated from unity for the different studied prepared bearing solutions as shown Table.5.

**Table 2:** Activity concentrations (Bq/ Kg) of  $^{238}\text{U}$ ,  $^{235}\text{U}$  and  $^{234}\text{U}$  for different sediment samples with different particle sizes.

Nuclide	Activity Concentrations (Bq/ Kg)								
	$^{238}\text{U}$			$^{235}\text{U}$			$^{234}\text{U}$		
Sample volume	63 $\mu\text{m}$	~ 33 $\mu\text{m}$	~ 8 $\mu\text{m}$	63 $\mu\text{m}$	~ 33 $\mu\text{m}$	~ 8 $\mu\text{m}$	63 $\mu\text{m}$	~ 33 $\mu\text{m}$	~ 8 $\mu\text{m}$
Sample code									
S1	14654.58 $\pm$ 267.45	16784.77 $\pm$ 189.59	18933.37 $\pm$ 158.22	661.67 $\pm$ 83.12	781.12 $\pm$ 93.44	871.23 $\pm$ 74.83	13982.49 $\pm$ 412.87	15849.67 $\pm$ 204.78	19001.52 $\pm$ 319.85
S2	1524.85 $\pm$ 109.45	1744.78 $\pm$ 98.59	1869.68 $\pm$ 111.71	71.08 $\pm$ 9.53	81.18 $\pm$ 16.83	85.72 $\pm$ 12.61	1471.41 $\pm$ 144.88	1695.07 $\pm$ 124.62	1883.22 $\pm$ 167.81
S3	1900.42 $\pm$ 107.15	2127.69 $\pm$ 167.61	2467.9 $\pm$ 77.39	92.55 $\pm$ 6.17	99.63 $\pm$ 24.16	113.81 $\pm$ 15.33	1839.84 $\pm$ 144.08	2092.42 $\pm$ 212.03	2583.83 $\pm$ 101.04
S4	13569.76 $\pm$ 367.46	14671.95 $\pm$ 612.99	16347.81 $\pm$ 812.09	644.09 $\pm$ 49.81	668.16 $\pm$ 104.91	751.05 $\pm$ 58.22	13109.02 $\pm$ 404.15	14271.9 $\pm$ 599.02	16512.19 $\pm$ 499.73

**Table 3:** Activity Ratios of  $^{238}\text{U} / ^{235}\text{U}$  and  $^{238}\text{U} / ^{234}\text{U}$  for different sediment samples with different particles sizes.

Nuclide	Activity Ratio					
	$^{238}\text{U} / ^{235}\text{U}$			$^{238}\text{U} / ^{234}\text{U}$		
Sample volume	63 $\mu\text{m}$	~ 33 $\mu\text{m}$	~ 8 $\mu\text{m}$	63 $\mu\text{m}$	~ 33 $\mu\text{m}$	~ 8 $\mu\text{m}$
Sample code						
S1	22.15	21.49	21.73	1.05	1.06	1.00
S2	21.45	21.49	21.81	1.04	1.03	0.99
S3	20.53	21.36	21.68	1.03	1.02	0.96
S4	21.07	21.96	21.77	1.04	1.03	0.99

Percents of Leachates quantities of different isotopes for different samples with different grain sizes are listed in Table.6. As shown in Table.6 values of leaching percent is nearly constant for the same sample type and no significant variation in the leaching percent has been found with decreasing of the sample grain size. Although the leaching percent is not affected by the sample grain size yet leaching quantities is generally increased for the same sample type at the smallest grain size as shown in Table.4 which recommends that in the leaching process minimum grain size is required to extract uranium from different ores.

**Table 4:** Activity concentrations (Bq/ L) of  $^{238}\text{U}$ ,  $^{235}\text{U}$  and  $^{234}\text{U}$  for different bearing solutions prepared from different samples with different particle sizes.

Nuclide	Activity Concentrations (Bq/ L)								
	$^{238}\text{U}$			$^{235}\text{U}$			$^{234}\text{U}$		
Sample volume	63 $\mu\text{m}$	~ 33 $\mu\text{m}$	~ 8 $\mu\text{m}$	63 $\mu\text{m}$	~ 33 $\mu\text{m}$	~ 8 $\mu\text{m}$	63 $\mu\text{m}$	~ 33 $\mu\text{m}$	~ 8 $\mu\text{m}$
Sample code									
S1	4853.60 $\pm$ 88.13	5631.29 $\pm$ 101.56	6230.97 $\pm$ 48.13	217.76 $\pm$ 17.41	262.07 $\pm$ 21.09	296.31 $\pm$ 18.76	5064.46 $\pm$ 233.02	5932.53 $\pm$ 180.58	6990.66 $\pm$ 135.82
S2	488.87 $\pm$ 51.04	554.32 $\pm$ 33.98	606.34 $\pm$ 45.07	23.44 $\pm$ 2.91	26.07 $\pm$ 4.02	27.47 $\pm$ 1.93	515.73 $\pm$ 38.04	595.99 $\pm$ 56.22	678.15 $\pm$ 87.23
S3	597.87 $\pm$ 14.85	677.46 $\pm$ 36.04	804.78 $\pm$ 23.64	29.67 $\pm$ 3.65	32.72 $\pm$ 2.76	36.29 $\pm$ 1.9	658.48 $\pm$ 44.03	757.67 $\pm$ 61.58	941.55 $\pm$ 76.82
S4	4617.79 $\pm$ 73.86	5053.02 $\pm$ 106.73	5541.91 $\pm$ 88.49	218.93 $\pm$ 9.67	231.65 $\pm$ 18.48	259.64 $\pm$ 20.51	5035.17 $\pm$ 188.39	5416.19 $\pm$ 124.52	6372.05 $\pm$ 176.44

**Table 5:** Activity Ratios of  $^{238}\text{U}/^{235}\text{U}$  and  $^{238}\text{U}/^{234}\text{U}$  for different bearing solutions

Nuclide	Activity Ratio					
	$^{238}\text{U}/^{235}\text{U}$			$^{238}\text{U}/^{234}\text{U}$		
Sample volume	63 $\mu\text{m}$	~ 33 $\mu\text{m}$	~ 8 $\mu\text{m}$	63 $\mu\text{m}$	~ 33 $\mu\text{m}$	~ 8 $\mu\text{m}$
Sample code						
S1	22.29	21.49	21.03	0.96	0.95	0.89
S2	20.85	21.27	22.07	0.95	0.93	0.89
S3	20.15	20.71	22.17	0.91	0.89	0.85
S4	21.09	21.81	21.34	0.92	0.93	0.87

**Table 6:** Leaching percent of  $^{238}\text{U}$ ,  $^{235}\text{U}$  and  $^{234}\text{U}$  for different bearing solutions.

Nuclide	Leaching Percent								
	$^{238}\text{U}$			$^{235}\text{U}$			$^{234}\text{U}$		
Sample volume	63 $\mu\text{m}$	~ 33 $\mu\text{m}$	~ 8 $\mu\text{m}$	63 $\mu\text{m}$	~ 33 $\mu\text{m}$	~ 8 $\mu\text{m}$	63 $\mu\text{m}$	~ 33 $\mu\text{m}$	~ 8 $\mu\text{m}$
Sample code									
S1	33.12	33.55	32.91	32.91	33.55	34.01	36.22	37.43	36.79
S2	32.06	31.77	32.43	32.98	32.11	32.05	35.05	35.16	36.01
S3	31.46	31.84	32.61	32.06	32.84	31.89	35.79	36.21	36.44
S4	34.03	34.44	33.9	33.99	34.67	34.57	38.41	37.95	38.59

Also Table.6 shows that values of leaching percent for  $^{234}\text{U}$  has highest percent of leaching quantities while these values for  $^{238}\text{U}$  and  $^{235}\text{U}$  are close to each other, this explains the occurring of disequilibrium in leachates. The reason for the higher  $^{234}\text{U}$  concentrations in leachates is due to  $\alpha$ - recoil process which enhances the mobilization and solubility of the decay product of  $^{234}\text{U}$  relative to the parent ( $^{238}\text{U}$ ). The enrichment in  $^{234}\text{U}$  is accordingly related to the crystal damage and leaching, which are the main mechanisms for the  $^{238}\text{U}/^{234}\text{U}$  disequilibrium (Ioannidou, 2011).

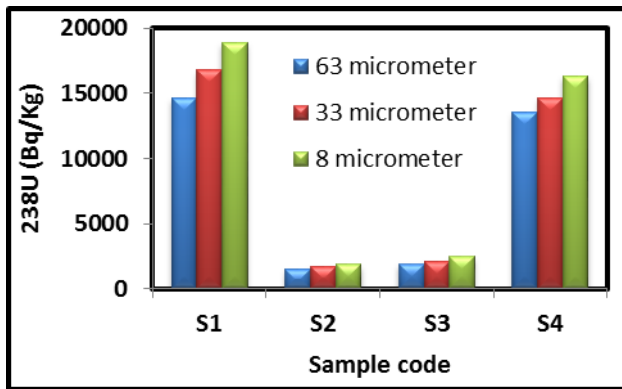
Fig.1. Uranium isotopes activity concentrations for different solid samples and the corresponding bearing solutions prepared from different samples with different grain sizes. corresponding bearing solutions (Bq/L), a&b for  $^{238}\text{U}$ , c&d for  $^{235}\text{U}$  and e&f for  $^{234}\text{U}$ .

As shown in Fig.1 activity concentration of all isotopes increased as the grain size of each sample is decreased this is in agreement with previous work (Karen, 1976).

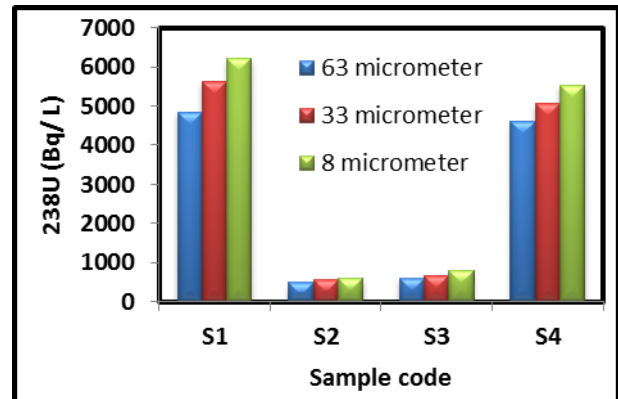
Disproportions between sample grain size and detected uranium for the same sample may be due to the large grain size of the sample working as a barrier facing the gamma rays causing gamma attenuation as a result of gamma interactions within the sample before reaching the detector. Attenuation of gamma rays has been attributed to density and chemical composition of the sample (Khater and Ebaid, 2008).

Fig.2. Average percent of different grain sizes for uranium isotopes contribution to the total uranium activity in different solid samples and their corresponding bearing solutions.

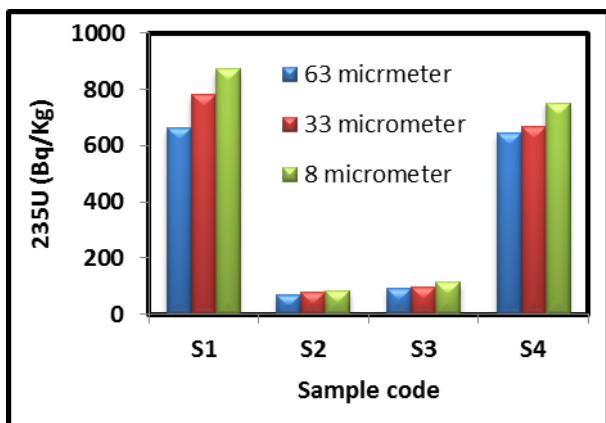
The rock solvent interaction produces many effects on uranium leaching quantity, but this does not explain why each isotope has unlike value compared to the other isotopes.  $^{234}\text{U}$  is an alpha decay product of  $^{238}\text{U}$  although they have activity equilibrium in solid samples however they are in disequilibrium in bearing solutions prepared from the same samples. The combined effects of diffusion and direct alpha recoil out of the solid matrix grain can induce  $^{234}\text{U}$  &  $^{238}\text{U}$  disequilibrium (Fernando, 1998).



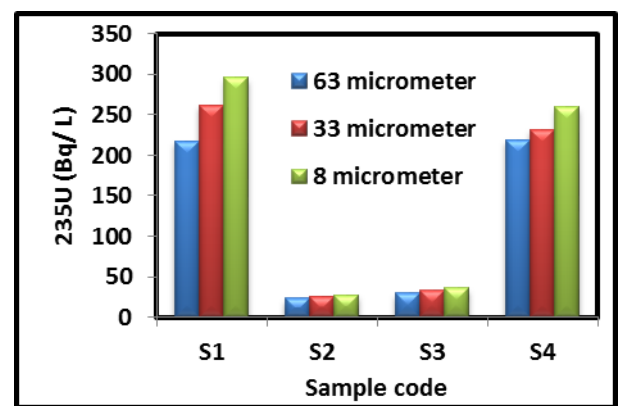
(a)



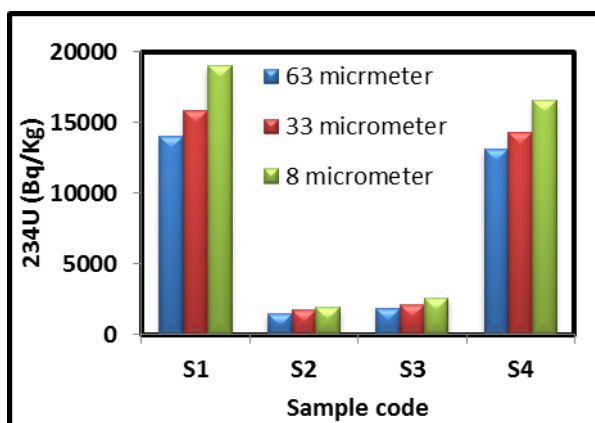
(b)



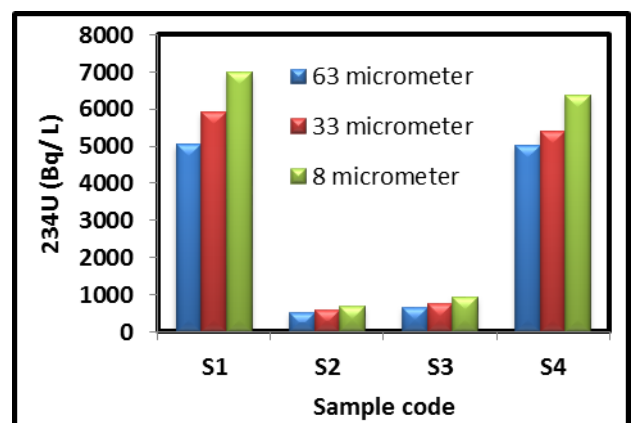
(c)



(d)



(e)



(f)

Fig. 1: Activity concentrations for different solid samples with different grain sizes (Bq/Kg) and the

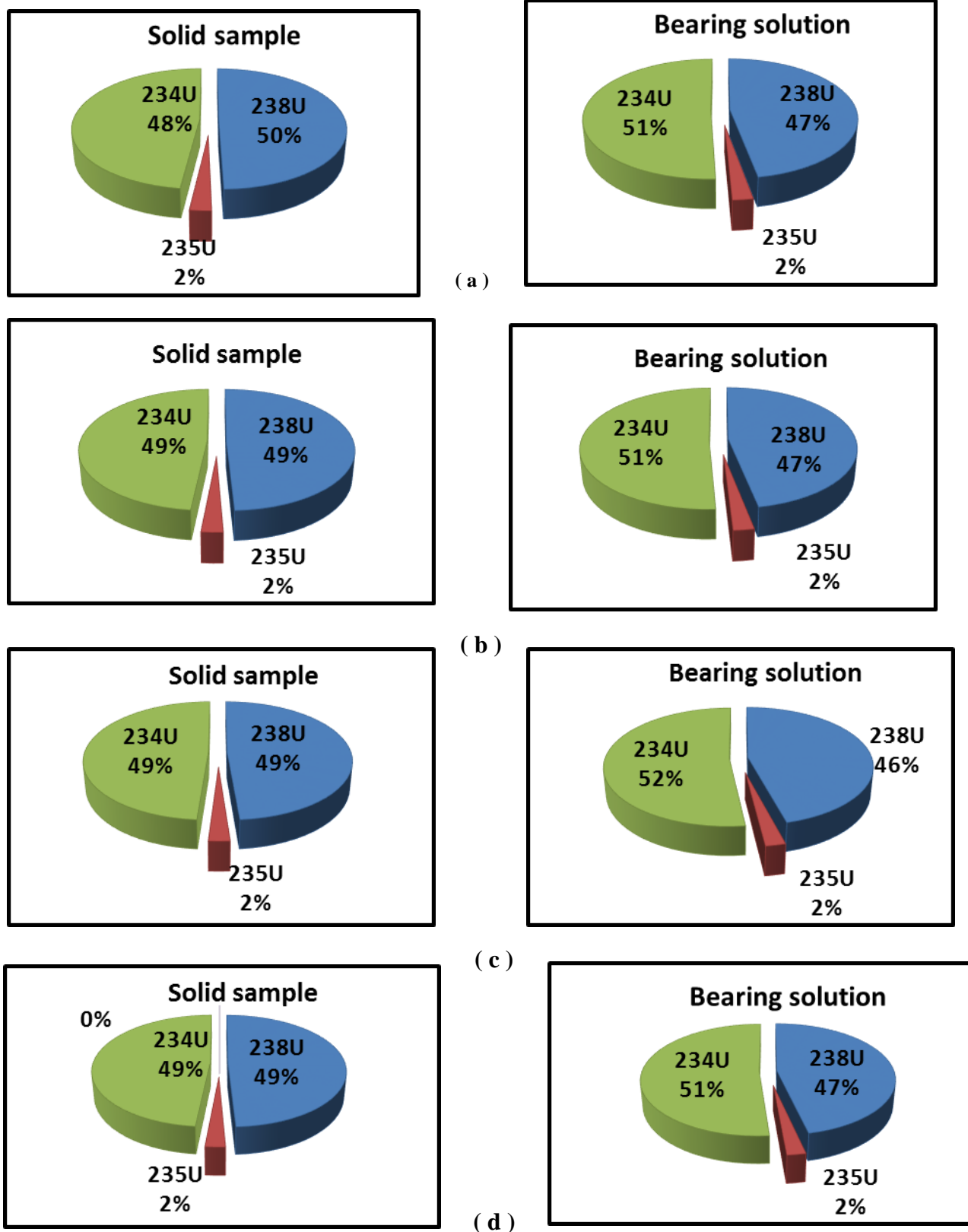


**Fig. 2:** Average activity contributions of uranium isotopes a, b, c and d for different solid samples and their corresponding bearing solutions S1, S2, S3 and S4 respectively.

## 5.2. Statistical analysis:

Heavy metals percent have been determined for different samples at different grain sizes using EDX instrument and listed in Table. 7.

**Table 7:** Element percent at different grain sizes for studied sedimentary samples.

Sample code	Grain size	Element%				
		Mg	Al	Si	Mn	Fe
S 1	~ 63 $\mu\text{m}$	6.55	1.95	5.67	0.98	3.44
	~ 33 $\mu\text{m}$	6.21	2.48	6.31	1.2	5.16
	~ 8 $\mu\text{m}$	5.52	3.16	12.85	2.48	7.16
S 2	~ 63 $\mu\text{m}$	2.11	4.19	13.99	0.96	0.93
	~ 33 $\mu\text{m}$	1.45	6.6	28.77	2.09	3.09
	~ 8 $\mu\text{m}$	1.27	8.82	37.53	3.81	7.66
S 3	~ 63 $\mu\text{m}$	1.55	3.08	5.44	1.66	29.89
	~ 33 $\mu\text{m}$	1.1	4.01	7.58	4.03	55.02
	~ 8 $\mu\text{m}$	0.98	5.51	12.12	4.48	62.76
S 4	~ 63 $\mu\text{m}$	2.18	6.44	13.67	6.89	2.96
	~ 33 $\mu\text{m}$	1.76	9.18	19.86	9.77	6.14
	~ 8 $\mu\text{m}$	1.3	14.06	24.21	11.06	10.48

Multivariate Pearson Correlation Coefficient values of uranium and heavy metals in the studied sediment samples were carried out and listed in Tables. 8, 9 and 10 for different grain sizes of 63, 33 and 8  $\mu\text{m}$ .

**Table 8:** calculated correlations between uranium and heavy metals in different samples for 63  $\mu\text{m}$  grain size.

Variables	Mg	Al	Si	Mn	Fe	U
Mg	1	-0.606	-0.457	-0.324	-0.397	0.675
Al	-0.606	1	0.826	0.872	-0.303	0.104
Si	-0.457	0.826	1	0.500	-0.634	-0.063
Mn	-0.324	0.872	0.500	1	-0.197	0.478
Fe	-0.397	-0.303	-0.634	-0.197	1	-0.492
U	0.675	0.104	-0.063	0.478	-0.492	1

**Table 9:** calculated correlations between uranium and heavy metals in different samples for 33  $\mu\text{m}$  grain size.

Variables	Mg	Al	Si	Mn	Fe	U
Mg	1	-0.613	-0.523	-0.463	-0.412	0.649
Al	-0.613	1	0.743	0.807	-0.343	0.096
Si	-0.523	0.743	1	0.204	-0.527	-0.292
Mn	-0.463	0.807	0.204	1	-0.008	0.369
Fe	-0.412	-0.343	-0.527	-0.008	1	-0.519
U	0.649	0.096	-0.292	0.369	-0.519	1

**Table 10:** calculated correlations between uranium and heavy metals in different samples for 8  $\mu\text{m}$  grain size.

Variables	Mg	Al	Si	Mn	Fe	U
Mg	1	-0.624	-0.446	-0.489	-0.425	0.694
Al	-0.624	1	0.561	0.912	-0.288	0.057
Si	-0.446	0.561	1	0.173	-0.529	-0.372
Mn	-0.489	0.912	0.173	1	-0.117	0.288
Fe	-0.425	-0.288	-0.529	-0.117	1	-0.539
U	0.694	0.057	-0.372	0.288	-0.539	1

As shown in the above data, the correlation between U and different heavy metals are:

- Positive correlation with Mg for different grain sizes, independent on grain size this approves the hosting of uranium by magnesite.
- Positive correlation with Mn and weak correlation with Al each correlation decreases as grain size is decreased, this matches positive correlation between Mn and Al which increased as the grain size is decreased.
- Negative correlation with each of Si & Fe which decreases as the grain size is decreased.

The above characteristics illustrate the installation of uranium inside the different minerals of the studied samples:

Where knowledge about chemical composition of the surface region of sediments is poor due to micron-thick coatings of secondary mineral phases and resistant organic materials that commonly occur on sediment surfaces (James *et al.*, 2004).

Uranium was introduced to dolomite during the process of dolomitization associated with magnesium carbonate and migrated out during the process of dedolomitization and the formation of magnesite with high

uranium content the produced laterites either grey (Al) soil or brown (Fe) soil are good adsorbent for uranium and other heavy metals (Ibrahim *et al.*, 2011).

The neutral to slightly acidic pH of the lithological materials also favoured strong adsorption on oxide and hydroxides of Fe and Mn as well as clay minerals (Satya and Jim, 2013).

#### Conclusions:

In the present study the levels of uranium isotopes are determined through the study of four selected sediment rock samples and uranium bearing solutions prepared from the same samples using Gamma-spectrometry. The results of activity concentrations of the different isotopes in all samples are presented and indicate that:

- Detected uranium activity concentrations of different isotopes increased as the sample grain size decreases.
- $^{238}\text{U}$  &  $^{234}\text{U}$  are in equilibrium in the studied solid sample, but they are in disequilibrium in the bearing solutions.
- Percent of leaching quantities indicates that  $^{234}\text{U}$  is the most leaching uranium isotopes compared to  $^{238}\text{U}$  &  $^{235}\text{U}$

Finally fine grain size is recommended for uranium leaching process to produce appropriate uranium quantities.

#### References

- Benedik L., H. Pintar, A. R. Byrne, 1999. The leachability of some natural and man-made radionuclides from soil and sediments on acid attack, *Journal of Radioanalytical and Nuclear Chemistry*, Vol. 240, No. 3, 859-865.
- Cecilia Edsfieldt and Joanne Femlund, Division of Engineering Geology, 2000. Differences in Radium and Uranium Distribution in Quaternary Deposits, Royal Institute of Technology International Radon Symposium.
- Fernando Brenha Riberio, 1998. Simultaneous Diffusion of Isotopes from a Radioactive Series in Homogeneous And Isotopic Solids, *Radiation Measurements* Vol. 29, No. 1, pp. 9 -18.
- El Aassy, E., Mohamed M. El Galy, Afaf A. Nada, Mohamed G. El Feky, Thanaa M. Abd El Maksoud, Shadia M. Talaat, Eman M. Ibrahim, 2011. Effect of alteration processes on the distribution of radionuclides in uraniferous sedimentary rocks and their environmental impact, southwestern Sinai, Egypt. *J Radioanal Nucl Chem* 289, 173–184, <http://dx.doi.org/10.1007/s10967-011-1059-1>.
- IAEA, 1987. Preparation and Certification of IAEA Gamma Spectrometry Reference Materials, RGU-1, RGTh-1 and RGK-1. International Atomic Energy Agency. Report- IAEA /RL /148.
- IAEA, 2001. Manual of acid in situ leach uranium mining technology, International Atomic Energy Agency. Nuclear Fuel Cycle and Materials Section.
- Ioannidou A., I. Samaropoulos, M. Efstathiou, I. Pashalidis, 2011. Uranium in ground water samples of Northern Greece *J Radio analytical and Nuclear Chemistry* 289:551 -555 DOI 10.1007/s10967-011-1115.
- James A. Davis, David E. Meece, Matthias Kohler, and Gary P. Curtis 2004. Approaches to surface complexation modeling of Uranium (VI) adsorption on aquifer sediments, *Geochimica et Cosmochimica Acta*, Vol. 68, No. 18, pp. 3621–3641.
- Jibiri, N.N., P. I. Farai, , K.S. Alausa, 2007. Estimation of annual effective dose due to natural radioactive elements in ingestion of food stuffs in tin mining area of Jos Plateau, Nigeria. *J. Environ. Radioact.* 94, 31–40.
- Khater A. E. M., Y. Y. Ebaid, 2008. A simplified gamma-ray self-attenuation correction in bulk samples. *Applied Radiation and Isotopes*; 66(3):407-413.
- Karen J. Wenrich- Verbeek, 1976. United States Department of the Interior Geological Survey Water and Stream-Sediment Sampling Techniques for Use in Uranium Exploration Open-File Report' 76-77.
- Maria Gavrilescu, Lucian Vasile Pavel, Igor Cretescu, 2009. Characterization and remediation of soils contaminated with uranium *Review Journal of Hazardous Materials*. 163, 475–510.
- Ramebäck H., A. Vesterlund, A. Tovedal, U. Nygren, L. Wallberg, E. Holm, C. Ekberg and G. Skarnemark, 2010. The Jackknife as an Approach for Uncertainty Instruments and Methods in Physics Research B: Beam Interactions with Materials and Atoms. 268: 2535-2538.
- Satya P. Singh and M. Jim Hendry, 2013. Solid-Phase Distribution and Leaching Behaviour of Nickel and Uranium in a Uranium Waste-Rock Piles, *Water Air Soil Pollut*, 224:1360 DOI 10.1007/s11270-012-1360-9.
- Sutherland, R.A., E. DeJong, 1990. Statistical analysis of gamma-emitting radionuclide concentrations for three fields in Southern Saskatchewan. *Canada Health Phys.* 58 (4), 417–428.
- Tucker, M.E., 2003. *Sedimentary rocks in the field: John Wiley & sons*, Third Edition, pp: 234.



- U.S. Department of Energy Office of Environmental Management 2001: Characteristics of Uranium and Its Compounds, Depleted Uranium Hexafluoride Management Program.
- Yokoyama Y, C. Falguères, F. Sémah, T. Jacob and R. Grün, 2008. Gamma-Ray Spectrometric Dating of Late Homo Erectus Skulls from Ngandong and Sambungmacan, Central Java, Indonesia. *Journal of Human Evolution*. 55: 274–277.
- Yücel, H., Solmaz A.N., Köse E. and D. Bor, 2010. Methods for Spectral Interference Corrections for Direct Measurements of  $^{234}\text{U}$  and  $^{230}\text{Th}$  in Materials by Gamma-Ray Spectrometry. *Radiation Protection Dosimetry*. 138: 264–277.